

**Micropollutant removal in real WW by photo-Fenton (circumneutral and acid pH)  
with BLB and LED lamps**

N. López-Vinent, A. Cruz-Alcalde, C. Gutiérrez, P. Marco, J. Giménez\*, S. Esplugas

*Department of Chemical Engineering and Analytical Chemistry, Faculty of Chemistry,*

*Universitat de Barcelona, C/Martí i Franqués 1, 08028 - Barcelona, Spain. Tel:*

*+34934021293. Fax: +34934021291*

\*Corresponding Author: [j.gimenez.fa@ub.edu](mailto:j.gimenez.fa@ub.edu)

**ABSTRACT**

In this study, photo-Fenton treatment was performed to remove a target compound (propranolol, PROP) from wastewaters of secondary effluents coming from WWTP. Two different radiation sources were tested: BLB and UV-A LEDs, which implies low electrical power and no mercury content. The differences observed in the PROP removal with both lamps may be due to the different radiation distribution, absorption inside the reactor, emission angle and wavelength emission, which are key parameters in the radiation field of the photoreactor. Four wastewaters (IFAS, MBR, CAS and CAS-NE) and ultrapure water were tested to determine the influence of water matrix. Instead the propranolol degradation using UV-A LEDs was smaller than using BLB lamps, in ultrapure water the degradation was very similar. The matrices with more organic matter and turbidity achieved low propranolol removals due to the competition for hydroxyl radicals and the effect of the light scattering. In addition, photo-Fenton at neutral pH (to avoid the acidification/basicification) was also carried out using two chelating agents

(EDDS and EDTA). Two molar ratios ligand-Fe(II) were tested (1:1 and 1.5:1). EDDS with L:Fe(II) molar ratio 1:1 was selected based on studies of MP degradation, biodegradability and toxicity. Comparisons between conventional photo-Fenton and photo-Fenton with EDDS-Fe(II) were performed with UV-A LEDs. For Milli-Q and IFAS best results were achieved in conventional photo-Fenton (32.9% for IFAS instead of 14.3% in EDDS-Fe(II)). Contrary, for the MBR, CAS and CAS-NE the best results were shown for EDDS-Fe(II) photo-Fenton. In IFAS, biopolymers and humic substances were the responsible of the different behavior of IFAS than other WW. Finally, for conventional photo-Fenton, dark Fenton plays an important role during the first 30 s, then, photo-Fenton controls the process. For circumneutral photo-Fenton, dark Fenton is not so important during the initial time. These observations have been corroborated by different kinetic fittings for different reaction times.

## **KEYWORDS**

Photo-Fenton, Wastewater matrix, Circumneutral pH, UV-A LED, Propranolol

## **1. Introduction**

Nowadays, there is a concern on the occurrence of micropollutants (MPs) in effluents of municipal wastewater treatment plants (WWTP) [1-8]. For instance, in Athens (Greece) an important amount of medicines and antibiotics in WW effluents were detected [3], 79 different MPs were identified in WWTPs of Swedish [4] and pharmaceuticals in the surface were found in some places in USA [5]. These compounds can enter the environment causing untoward human health and ecological effects [6]. The potential for entering in the environment of these compounds is a consequence of their incomplete removal in conventional WWTPs [7, 8].

Accordingly, with the future law requirements and to protect the ecosystems and water resources, additional treatments ought to be carried out [9]. Diverse works to remove MPs are based in Advanced Oxidation Processes (AOPs). Some authors indicated the efficiency of these treatments in the elimination of organic and recalcitrant compounds [6, 9, 19-25]. In this study, propranolol (PROP) was used as reference compound. This compound is used to treat cardiovascular diseases and is a non-selective  $\beta$ -blocker and it is the most frequent  $\beta$ -blocker found in aquatic environment [10]. PROP has been detected in the environment, for instance in wastewaters [11] or in rivers with a range of concentrations between 0.1-7.3 ng/L [12]. This compound was also detected for by Deo in a surface waters with a concentration of 53 ng/L [5]. The occurrence in wastewaters includes private household, effluents from hospitals and retirement homes and pharmaceutical plant wastewater [13]. Propranolol has been detected in a different aquatic environments and countries, such as Spain, Croatia, France, Serbian, Bosnian and China [12, 14-17]. Concerning ecotoxicology, some studies indicate that aquatic organisms present high sensitivity to PROP [18]. Among AOPs, the photo-Fenton treatment has been demonstrated its efficiency in the elimination of a variety of compounds: pesticides [19], dyes [20], insecticides [21], pharmaceuticals [22, 23], humic acids [24] and PCBs [25], among others.

Nevertheless, there are some drawbacks related to the conventional photo-Fenton process. The costs associated with photo-reactor investment, electrical cost of lamps and reagents are the principal disadvantages for full-scale application for photo-Fenton [26, 27]. Chemicals to adjust pH (to avoid iron precipitation) and subsequent neutralization and hydrogen peroxide ( $H_2O_2$ ) consumption are the main costs related to reagents [28, 29].

Several ligands for the iron complexation, to work at circumneutral pH, have been studied to overcome the drawbacks of photo-Fenton at acidic pH [29, 30, 31]. On the other hand, the costs associated to energy consumption could be decreased using light-emitting diodes (LEDs) as a source of radiation. In recent years, the studies with the use of LEDs in AOPs have increased [32, 33] because LEDs show many advantages such as low power consumption, long lifetime (up to 26,000 h), no overheating and no mercury content [32-41].

Other important item to consider, due to the water scarcity, is the possibility of water reuse. In this way, more data are needed to know the behavior of different AOPs, with water matrices coming from WWTPs. In this way, four matrices of secondary effluents from WWTPs were used and compared with Milli-Q water: Integrated Fixed-Film Activated Sludge (IFAS), Membrane Bioreactor (MBR), Conventional Activated Sludge (CAS) and the same process with nutrient elimination (CAS-NE) with 70% elimination of nitrogen and phosphorus. IFAS and CAS showed high amount of organic matter and turbidity (see Table 1). However, MBR and CAS-NE, presented low values of these parameters. IFAS was the dirtiest matrix with values approximately of  $52 \text{ mg C}\cdot\text{L}^{-1}$  of total organic carbon (TOC) followed by CAS presenting  $38 \text{ mg C}\cdot\text{L}^{-1}$  of TOC. CAS-NE and MBR shown similar values of TOC (around  $13 \text{ mg C}\cdot\text{L}^{-1}$ ) but different values of turbidity, which is an important parameter in this comparison.

Summarizing, this paper is focused on the study of the efficiency of the photo-Fenton treatment, using two different light sources (Black-light blue lamps (BLB) and LEDs), in the propranolol (PROP) degradation in four secondary wastewater matrices from two WWTPs. The effect of iron chelates (EDTA/ EDDS) at different molar ratios (Fe(II)-

Ligand) using UV-A LED was tested in the four wastewater matrices. Biodegradability and efficiency were also evaluated to determine the capability of the photo-Fenton process at circumneutral pH.

## **2. Methodology**

### *2.1. Chemicals*

Propranolol hydrochloride (PROP) from Sigma-Aldrich was used as a target compound. *S,S'*-ethylenediamine-*N-N'*-disuccinic acid trisodium salt (EDDS-Na) solution from Sigma-Aldrich and ethylenediaminetetracetic acid (EDTA) from Panreac Quimica Inc. were used as a chelating agents. In photo-Fenton experiments hydrogen peroxide (30% w/w) from Sigma-Aldrich and ferrous sulfate ( $\text{FeSO}_4 \cdot 7\text{H}_2\text{O}$ ) from Panreac Quimica were used. Acetonitrile and orthophosphoric acid (Panreac Quimica) were used as a mobile phase for HPLC. Sodium hydroxide (NaOH) and sulphuric acid ( $\text{H}_2\text{SO}_4$ ) (both from Panreac Quimica Inc) were employed for the initial pH adjustments and subsequently neutralization, respectively.

### *2.2. Secondary effluents samples*

Two secondary effluents (after the biological treatment) from two different Wastewater Treatment Plants (WWTPs) of Catalonia (Spain) were tested in this study. The characteristics of these wastewaters (WW) are shown in Table 1. The samples of the secondary effluent, were filtered with conventional laboratory paper to remove the largest particles. One WWTP has two parallel secondary treatments which include IFAS and MBR. The second one includes CAS and CAS-NE.

**Table 1.** Physicochemical parameters of secondary effluent samples.

<b>Parameter</b>	<b>IFAS</b>	<b>MBR</b>	<b>CAS</b>	<b>CAS-NE</b>
pH	7.8	7.7	8.0	7.5
Turbidity (NTU)	18.5	0.5	20.1	2.6
UV <sub>254</sub> (cm <sup>-1</sup> )	50.3	17.4	48.9	24.6
TOC (mg C · L <sup>-1</sup> )	51.1	13.6	37.9	13.3
DOC (mg C · L <sup>-1</sup> )	21.7	13.3	18.7	13.2
Total alkalinity (mg CaCO <sub>3</sub> ·L <sup>-1</sup> )	469.4	208.3	449.1	275.0
Cl <sup>-1</sup> (mg·L <sup>-1</sup> )	543.0	565.2	486.0	464.4
SO <sub>4</sub> <sup>2-</sup> (mg·L <sup>-1</sup> )	196.8	187.8	175.2	199.5
N-NO <sub>2</sub> <sup>-</sup> (mg·L <sup>-1</sup> )	0.2	0.2	0.1	0.3
N-NO <sub>3</sub> <sup>-</sup> (mg·L <sup>-1</sup> )	0.3	8.4	0.3	8.3

### 2.3. Photo-Fenton experiments

All experiments were performed in a 2L Pyrex-jacketed thermostatic photoreactor (inner diameter 11 cm; height 23 cm). A BLB lamp (Philips TL 8W, 08 FAM, wavelength range 290-400 nm with a maximum at 365 nm), covered with a quartz glass tube, was located at the center of the reactor. A hand-made lamp with eight LEDs (Intelligent LED solutions) arranged on an aluminum bar forming a spiral (to minimize the dark zones in the photoreactor) was also employed. The nominal power of each LED was 1.00 W, with 350 mA, irradiance angle of 125° and emission wavelength at 365 nm. The temperature of the solution was kept constant at 25 °C with a thermostatic bath (Haake C-40) and the solutions were magnetically stirred into the photoreactor.

To carry out the conventional photo-Fenton experiments, a solution of 0.18 mM of Fe(II) was prepared in water acidified at pH 2.8 ±0.2 with H<sub>2</sub>SO<sub>4</sub>. Then, PROP (0.19 mM = 50

mg/L) was added (this concentration was selected to assure accurate measurements of concentrations) and, finally hydrogen peroxide (4.41 mM = 150 mg/L) was added just before to run the experiment. These concentrations were selected because they achieved the best efficiency in PROP removal, according to previous experiments done in our laboratory. In the experiments at circumneutral pH, iron chelates (EDTA or EDDS) at two molar ratios (1:1 and 1:1.5) of L-Fe(II) were tested. Then, the pH of the EDTA solution was adjusted around 8.0 with NaOH 0.2 M to allow their dissolution due to the low solubility of this compound at acid pH. After the chelates were totally dissolved, Fe(II), H<sub>2</sub>O<sub>2</sub> and PROP were added to the solution using the same concentrations listed above. Samples were taken from the photoreactor at fixed times during one hour.

#### *2.4. Analytical methods*

HPLC (Infinity Series from Agilent) was used to determine the concentration of PROP. Acetonitrile and Milli-Q water adjusted at pH=3 by orthophosphoric acid (25:75) were employed. UV detector at 214 nm and a flow of 0.7 mL min<sup>-1</sup> were applied. The column used was SEA18 Teknokroma (250 x 4.6 mm i.d; 5µm particle size). Hydrogen peroxide (H<sub>2</sub>O<sub>2</sub>) consumption was followed by the metavanadate spectrophotometric method [42]. Total iron was determined by the o-phenantroline standardized procedure (ISO 6332) at 510 nm. Biochemical Oxygen Demand (BOD) was evaluated according to the 5210-standard method (see supplementary material for more information in section: Biochemical Oxygen Demand: Brief explanation of the process). The analysis of COD was done according the ASTM D1252-06 Standard Test Methods, consisting in the sample oxidation with potassium dichromate in excess, in an acid medium, with catalysts and at 150°C for 2h [43]. Toxicity assays were performed in Microtox M500 toxicity analyzer (Modern Water, UK) [43]. Size Exclusion Chromatography combined with

Organic Carbon Detection (SEC-OCD) was used to detect and quantify the different effluent organic matter (EfOM) present in the WW matrices tested [44] (more information can be found in Table S1 in supplementary information).

### **3. Results and discussion**

#### *3.1. Light sources comparison and effect of the matrix*

The degradation of PROP by conventional photo-Fenton ( $\text{pH} = 2.8 \pm 0.2$ ) with BLB and UV-A LED is shown in Fig.1. Four wastewater matrices were tested with UV-A LED (MBR, CAS-NE, CAS, IFAS). The experiments achieving the best and the worst results in PROP degradation with UV-A LED were also performed with BLB lamps. In addition, Milli-Q water was also tested to evaluate more accurately the influence of water matrix.

In the presence of UV-A LED, PROP degradation at 60 minutes was 100%, 52.1%, 50.6%, 40.2% and 32.9% for Milli-Q, MBR, CAS-NE, CAS and IFAS, respectively. While in the presence of BLB light source, PROP degradations reached were 100%, 95.3% and 68.8% for Milli-Q, MBR and IFAS, respectively. Thus, the same trend was followed with the two radiation sources and PROP removal decreases when TOC of water matrix increases. The percentage of standard deviation in photo-Fenton experiments did not exceed 5%. As can be observed in Fig.1, in the case of Milli-Q water similar PROP removal was achieved at 60 minutes for both, BLB and UV-A LED. Moreover, the kinetic constants obtained were very close ( $0.15 \text{ min}^{-1}$  for BLB and  $0.14 \text{ min}^{-1}$  for LEDs, after first 30 seconds and assuming first order kinetics). When real matrices were used, the differences between BLB and LEDs were higher. This can be related to radiation distribution and absorption inside the reactor. Thus, the emission angle for BLB is  $360^\circ$  and only  $125^\circ$  for LEDs, which implies different distribution of radiation and probably dark zones in the case of LEDs. This last hypothesis can be strengthened because LEDs



are punctual sources of light (see figure S1 in the supplementary information). In addition, although BLB presents the maximum peak at 365 nm, the emission range (290-400 nm) is wider than in LEDs (365-370 nm). Thus, depending on the absorption of different compounds in the real matrix their photolysis could be higher when BLB or LEDs are used. Probably in a complex system, such as a real matrix, the use of a light source with wider emission range favours the removal of different types of organic matter.

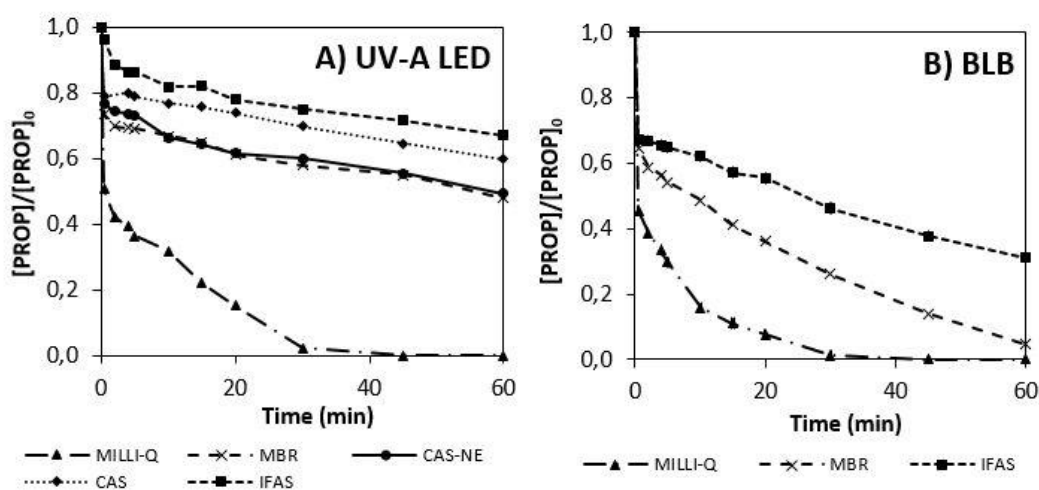


**Figure 1.** PROP degradation in different light sources by conventional photo-Fenton process.  $[\text{PROP}]_0 = 0.19 \text{ mM}$ ;  $[\text{Fe(II)}]_0 = 0.18 \text{ mM}$ ;  $[\text{H}_2\text{O}_2]_0 = 4.41 \text{ mM}$ .

Real wastewaters compared with ultrapure water are complex systems due to different physico-chemical parameters (turbidity, high Total Organic Carbon (TOC), colour, presence of ions, etc.). Thus, WW matrices do not favor the photolysis and there is a highest competition of hydroxyl radicals [45] due to the presence of organic compounds different of target compound. Figure 1 shows the influence of different matrices with UV-A LED. Thus, ultrapure water, which achieved the best results, presents a TOC of  $2 \mu\text{g/L}$  and obviously does not present ions or turbidity. Consequently, hydroxyl radicals only degrade the target pollutant and the byproducts of reaction, but no competition was

detected with other compounds of the matrix. Regarding the values of TOC, these decrease following the order IFAS, CAS, CAS-NE and MBR. Thus, less competition is provided for the radicals produced and higher removal of the target compound was achieved when values of TOC were lower. As obvious, the composition of each WW is different but several authors have determined the kinetic constants for the reaction between hydroxyl radicals and dissolved organic matter (DOM). These values are in the order  $10^8$ - $10^9$  L·molC<sup>-1</sup>·s<sup>-1</sup> [46-51], which can explain again the strong competition between organic matter present in WW and target compound for the hydroxyl radicals. Other important parameter influencing on PROP removal was turbidity due to light scattering. In this way, IFAS presents high turbidity and the highest TOC and, as a consequence, the lowest PROP removal. However, MBR and CAS-NE presented very close results in PROP degradation, achieving the highest removals of PROP, regarding wastewaters. In that case, their values of TOC and turbidity were the lowest. In the same way as the TOC, the dissolved organic carbon (DOC) influences on micropollutant degradation. The presence of an organic matter in solution can compete with target compound for hydroxyl radicals reducing the removal efficiency of the micropollutant. In addition, UV<sub>254</sub> is a spectroscopic property related to the presence of organic matter, particularly aromatic and unsaturated moieties which can also readily react with hydroxyl radicals. IFAS, which achieved lower PROP degradation, also showed the highest values of DOC and UV<sub>254</sub> and MBR, which shown the best PROP removal, the lowest. Finally, the effect of ions (Cl<sup>-</sup>, SO<sub>4</sub><sup>2-</sup>, N-NO<sub>2</sub><sup>-</sup>) was not significant, because their concentrations were similar in all treated WW. Nevertheless, when ultrapure water and wastewater were compared the effect of ions can appear. Alkalinity is an important indicator of (bi)carbonates concentration in WW. However, in conventional photo-Fenton, the alkalinity of the solution was neutralized when the matrix was acidified and then mixed.

Other inorganic ions can act as a scavenger of  $\cdot\text{OH}$ . The nitrite reacts with the hydroxyl radicals, producing nitrite radicals, with a second-order reaction rate of  $1.0 \cdot 10^{10} \text{ M}^{-1} \text{ s}^{-1}$  [52]. According to Benner and coworkers, the reaction rate of propranolol is  $1.0 \cdot 10^{10} \text{ M}^{-1} \text{ s}^{-1}$  [53]. Thus, the reaction rate for PROP and nitrite with  $\cdot\text{OH}$  is practically the same. However, as the nitrite concentration is lower than PROP the nitrite probably acts as a scavenger to a lesser extent in these experiments. Moreover, nitrite can produce hydroxyl radicals by photolysis (Eq. 1 and Eq. 2).



Nitrite absorbs radiation in the UV-A range (around 355 nm) [54] but its concentration in the four WW tested is very low. Thus, the equilibrium between generation and scavenging of hydroxyl radicals produces a stationary state in hydroxyl radicals concentration [54]. Regarding nitrates, in accordance with Buxton *et al.* [52]  $\text{NO}_3^-$  does not react with hydroxyl radicals. The photolysis of nitrates, giving  $\cdot\text{OH}$  radicals, has been studied in various works [55, 56, 57]. They mostly absorb in the UV-B (absorption maximum around 305 nm). However, LEDs used in this work emit in 365-370 nm range. Thus, the photolysis of nitrate is not possible. Finally,  $\text{Cl}^-$  reacts with hydroxyl radicals with a second-order reaction rate of  $43 \cdot 10^9 \text{ M}^{-1} \text{ s}^{-1}$  [52]. As mentioned above, the reaction rate of propranolol is  $1.0 \cdot 10^{10} \text{ M}^{-1} \text{ s}^{-1}$ , being higher than this one of chloride. Nevertheless, the concentration of chloride is 10 times higher than propranolol in the tested WW. Thus, the ion chloride probably acts as a scavenger of hydroxyl radicals. Thus, when ultrapure water and wastewaters were compared the results achieved presented significant differences due, in part, to the presence of ions in WW. However, according to Table 1 data, the ions concentrations are very close for the different WW tested. Consequently,

ions concentrations do not imply significant differences in the influence of the different WW matrices on PROP removal.

### 3.2. *photo-Fenton at circumneutral pH with LEDs*

#### 3.2.1. *Iron chelates*

An important parameter in photo-Fenton process when ligands (L) are used is the L-Fe molar ratio. A ratio L-Fe, higher than stoichiometric, is required experimentally to ensure a satisfactory chelation process [28]. Two ligands were tested (EDTA and EDDS) at two molar ratios L-Fe (1:1 and 1.5:1). The percentage of chelated iron with each condition was determined at 258 nm [28] with ultrapure water to avoid any interference. The results are shown in figure 2.

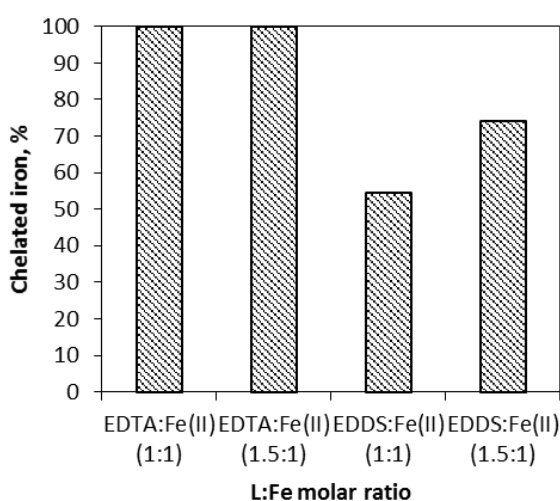


**Figure 2.** Percentage of iron chelates formed with two L:Fe(II) molar ratios tested. Calculated by absorbance at 258 nm.

Regarding Fig. 2, EDTA presents the 100% of chelated iron for both molar ratios 1:1 and 1.5:1. However, for EDDS the percentage of chelated iron is always lower than 100% and

that percentage increases with 1.5:1 molar ratio (54.4% and 74.0% for 1:1 and 1.5:1, respectively).

The decision on the best chelating agent and the best molar ratio L-Fe (II) also depends on the efficiency in the target compound degradation and the increase in the biodegradability. In this way, the results of PROP degradation are showed in figure 3. All the experiments presented in this section were performed in ultrapure water to avoid any interference.

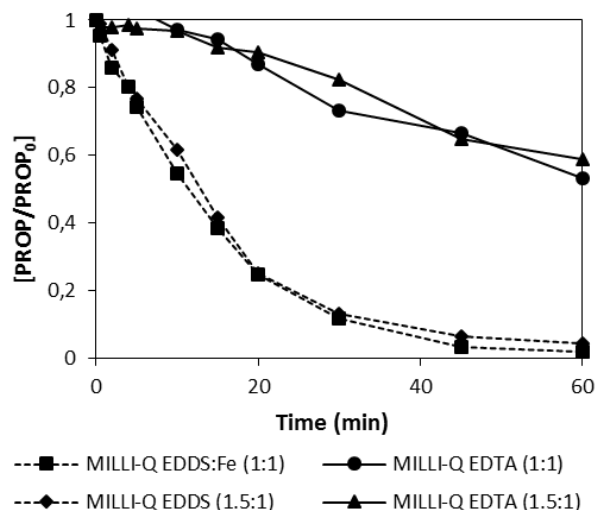


**Figure 3.** PROP degradation with EDTA and EDDS and two molar ratio L:Fe(II) (1:1 and 1.5:1) in ultrapure water.  $[PROP]_0 = 0.19$  mM;  $[Fe(II)]_0 = 0.18$  mM;  $[H_2O_2]_0 = 4.41$  mM. Radiation source: LEDs.

For both EDDS and EDTA, the same PROP degradation results were observed when two ratios were tested (Fig. 3). The pseudo-first order kinetic constants for EDDS-Fe(II) were  $0.07$  and  $0.06$   $\text{min}^{-1}$  for L-Fe(II) molar ratio of 1:1 and 1.5:1, respectively. For EDTA-Fe(II), the kinetic constant was  $0.01$   $\text{min}^{-1}$  for the two L-Fe molar ratios. Thus, EDDS runs better than EDTA in PROP degradation. 99.6% for EDDS and 47.3% for EDTA

after 60 minutes (molar ratio L-Fe(II) 1:1). The best molar ratio L-Fe(II) is 1:1, implying that less amount of chelating agent has to be used, which represents a decrease in effluent's TOC and in the cost associated at chelating agent. Moreover, PROP and chelates compete for hydroxyl radicals and this fact explains the efficiency decrease when L-Fe(II) ratio increases.

Other properties to take into account to select the best chelate are biodegradability and toxicity. Figure 4 shows that the biodegradability increase is higher for EDDS than EDTA. The results agree with the research works of different authors who investigated the replacement of EDTA to EDDS [29, 31]. Thus, EDDS is a more appropriate chelating agent than EDTA, because it is environmentally friendly, easily biodegradable and stable at neutral pH [38]. Finally, regarding to hazardousness, toxicity (*Vibrio fisheri*) was assessed for both EDTA and EDDS (molar ratio L-Fe(II) 1:1) The results were expressed with  $1/EC_{50}$ , being  $EC_{50}$  the value of sample dilution that kills 50% of bioluminescent bacteria population. The values obtained were 0.008 and 0.016 for EDDS and EDTA, respectively, indicating that EDTA is about 2 times more toxic than EDDS.

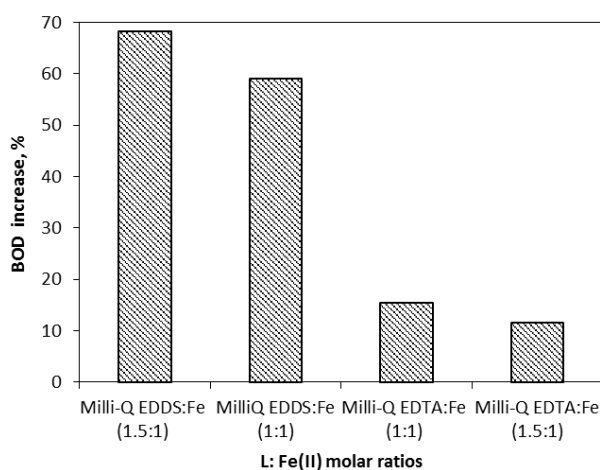


**Figure 4.** Percentage of BOD increase after treatment of EDTA and EDDS with 1:1 and 1.5:1 L-Fe(II) molar ratios.  $[PROP]_0 = 0.19$  mM;  $[Fe(II)]_0 = 0.18$  mM;  $[H_2O_2]_0 = 4.41$  mM.

### 3.2.2. Efficiency of EDDS-Fe(II) in different water matrices with LEDs

The efficiency of EDDS-Fe(II) complex was compared in the PROP degradation by photo-Fenton in the different water matrices previously used (see Fig. 5). The initial pH was the corresponding to each wastewater, around 7.5-8.0 (Table 1), and remained stable during the experiment.

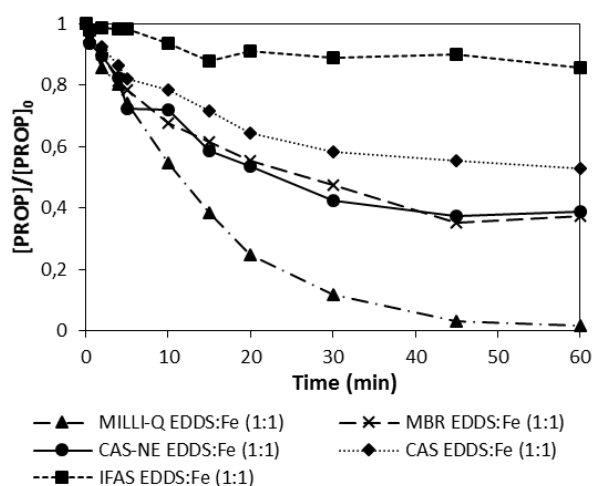


**Figure 5.** PROP degradation in different matrices by photo-Fenton, with LEDs, at circumneutral pH. EDDS:Fe(II) (1:1);  $[\text{PROP}]_0 = 0.19 \text{ mM}$ ;  $[\text{Fe(II)}]_0 = 0.18 \text{ mM}$ ;  $[\text{H}_2\text{O}_2]_0 = 4.41 \text{ mM}$ .

Regarding the percentages of PROP eliminated (60 minutes), they were 99.6, 62.7, 61.0, 47.0 and 14.3% for Milli-Q, MBR, CAS-NE, CAS and IFAS, respectively. As commented before, the PROP removal decreases when the TOC of WW increases. Thus, IFAS, with the highest TOC (see Table 1), shows the lowest degradation with only a 10% after 1 hour of experiment. This behavior points out the competition of the organic matter present in WW for the hydroxyl radicals and light.

During the reaction, an important parameter to follow is the total dissolved iron, because hydroxyl radicals attack PROP and organic matter of wastewaters but also the EDDS-Fe(II) complex. Figure 6 shows the total iron dissolved remaining in solution for each wastewater during the experiment.

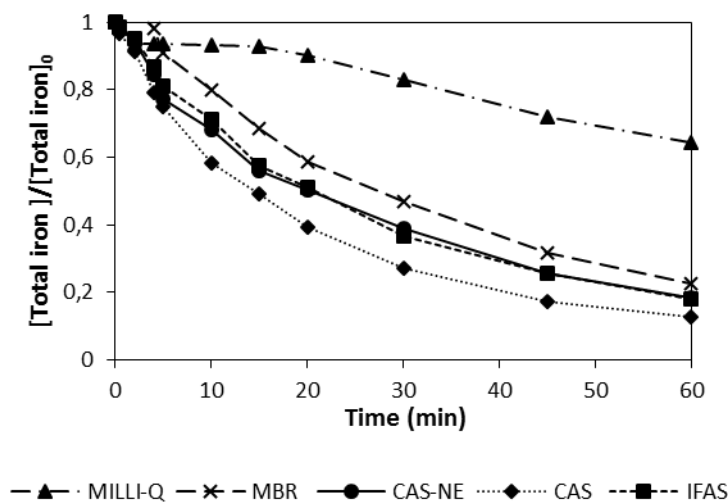


**Figure 6.** Total dissolved iron during the reaction of photo-Fenton catalyzed by EDDS-Fe(II) for each wastewater. EDDS:Fe(II) (1:1); [PROP]<sub>0</sub> = 0.19 mM; [Fe(II)]<sub>0</sub> = 0.18 mM; [H<sub>2</sub>O<sub>2</sub>]<sub>0</sub> = 4.41 mM.

As it can be observed in the figure 6, the iron remaining at the end of the treatment was lower when wastewaters were used. The values of total iron in solution at 60 minutes were between 10-25% of the total initial iron in solution in different wastewaters. However, when Milli-Q water was tested around 70% of total initial dissolved iron remained at the end of the experiment. The stability of the complexes can be affected by many parameters. In this sense, in Milli-Q water only target compound, their respective intermediates and chelating agent are present in the solution. Nevertheless, wastewater matrices are a complex system with different types of organic matter and other dissolved species. All this decrease the stability of the complexes making them more vulnerable to hydroxyl radicals.

In the same way that total dissolved iron was analyzed, the concentrations of H<sub>2</sub>O<sub>2</sub> for different wastewaters were monitored during the reaction. In supplementary material can be found a figure (Fig. S2) with hydrogen peroxide curves for each wastewater in conventional photo-Fenton and photo-Fenton catalyzed by EDDS-Fe(II) with LEDs.



The PROP removal at conventional photo-Fenton and photo-Fenton catalyzed by EDDS-Fe(II) is reported in Figure 7 in order to establish comparisons between the two systems.

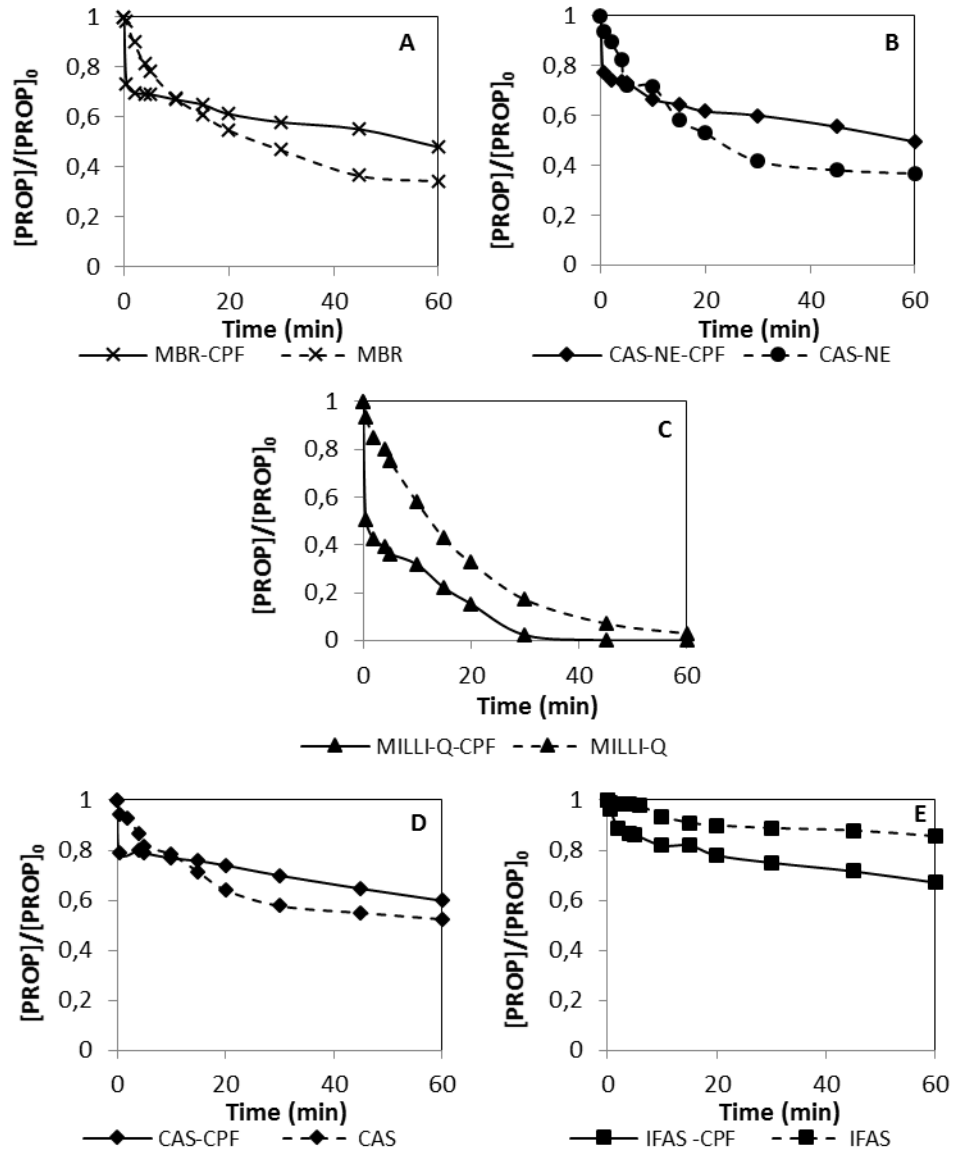


**Figure 7.** Degradation of PROP by conventional photo-Fenton (CPF) and photo-Fenton, with LEDs, catalyzed by EDDS-Fe(II) in different wastewaters. EDDS:Fe(II) (1:1);  $[\text{PROP}]_0 = 0.19 \text{ mM}$ ;  $[\text{Fe(II)}]_0 = 0.18 \text{ mM}$ ;  $[\text{H}_2\text{O}_2]_0 = 4.41 \text{ mM}$ .

In Figure 7 it is observed that, for all tested water matrices, there is a common trend, with lower TOC and DOC, higher conversion. Therefore, Milli-Q gives the best results and

IFAS the worst ones. This happens for both conventional photo-Fenton and photo-Fenton at circumneutral pH.

For a better comparison, different fittings were done and results are shown in Table 2.

The used data are these ones of the experiments presented in Figure 7.

**Table 2.** Values of kinetic constants for conventional photo-Fenton and photo-Fenton catalyzed by EDDS ( $k_1$ ,  $k_2$ ,  $k_3$  fitting to pseudo first order kinetics,  $k_4$  to zero order kinetic).

Kinetic constants	$k_1$	$k_2$	$R^2$	$k_3$	$R^2$	$k_4$
	( $\text{min}^{-1}$ )	( $\text{min}^{-1}$ )	$k_2$	( $\text{min}^{-1}$ )	$k_3$	(ppm/min)
MILLI-Q-CPF	1.354	0.135 $\pm 0.040$	0.92	0.136 $\pm 0.030$	0.92	0.022
MBR-CPF	0.621	0.006 $\pm 0.001$	0.96	0.0085 $\pm 0.006$	0.60	0.010
CAS-NE-CPF	0.525	0.007 $\pm 0.001$	0.92	0.0093 $\pm 0.005$	0.68	0.010
CAS-CPF	0.477	0.005 $\pm 0.001$	0.98	0.0065 $\pm 0.004$	0.68	0.008
IFAS-CPF	0.073	0.006 $\pm 0.002$	0.87	0.0064 $\pm 0.002$	0.82	0.006
MILLI-Q EDDS	0.129	0.058 $\pm 0.002$	0.99	0.0220 $\pm 0.002$	0.99	0.021
MBR-EDDS	0.038	0.021 $\pm 0.004$	0.96	0.0219 $\pm 0.004$	0.96	0.014
CAS-NE-EDDS	0.129	0.021 $\pm 0.005$	0.93	0.0220 $\pm 0.005$	0.93	0.014
CAS-EDDS	0.120	0.013 $\pm 0.003$	0.92	0.0135 $\pm 0.003$	0.91	0.010
IFAS-EDDS	0.025	0.003 $\pm 0.001$	0.83	0.0031 $\pm 0.001$	0.84	0.003

The kinetic constant  $k_1$  corresponds to the initial reaction rate and has been calculated for the initial 30 s of the experiment.  $k_2$  and  $k_3$  were calculated assuming pseudo-first order kinetics, according to eq. 3. For the fitting of  $k_2$  only the concentration-time data from 30 s to the end of the experiment have been used. While, for  $k_3$  fitting, the concentration-time data from time zero to the end of the experiment have been considered. In both cases, 45 min has been taken as the final time, because at this time the 100% of PROP degradation is achieved in Milli-Q water and conventional photo-Fenton.

$$\ln\left(\frac{c_f}{c_0}\right) = k \cdot t \quad \text{(Eq. 3)}$$

On the other hand,  $k_4$  indicates an average rate of PROP removal (would be equivalent to assume zero-order kinetics) and it has been estimated according to eq. 4.

$$k_4 = \frac{c_0 - c_f}{t} \quad \text{(Eq. 4)}$$

Where  $c_0$  is the initial PROP concentration (ppm),  $c_f$  is the final PROP concentration (ppm) and  $t$  is the time (min).

It should be noted that the kinetic constants that appear in table 2 will be used qualitatively trying to explain the shape of the graphs in Figure 7. Their absolute values do not matter as much as the comparison between them. Likewise, all these constants have been indicated to show the importance of choosing well the type of fitting and the intervals used.

From figure 7, it can be seen that, in conventional photo-Fenton and WW matrices, the concentration of PROP decreases quickly at the beginning of the experiment, during the first 30 seconds, and then decreases very slowly. From there it could be deduced that, in the initial 30 seconds, dark-Fenton controls the reaction rate. In addition it can be said that  $k_1$  decreases when TOC of WW increases. After this period, since the  $\text{Fe}^{2+}$  has already

passed practically everything to  $\text{Fe}^{3+}$ , photo-Fenton would be the controlling mechanism and the reaction rate becomes much slower. In fact, it is also observed in table 2 that  $k_1$  is much higher than  $k_2$  (in the case of MBR, CAS-NE and CAS is almost 100 times higher). In the case of IFAS, it is only 10 times higher for different reasons that will be discussed later.

In circumneutral photo-Fenton, one could say that the behavior is similar to a certain extent. In this case, the initial drop in the concentration of PROP is lower because  $\text{Fe}^{2+}$  is chelated. In fact, the  $k_1$  values in Table 2, for the same water matrix, are lower for circumneutral photo-Fenton. However, it is also observed that at the end of the experiment the curves flatten because the iron has already largely precipitated (see figure 6) and the photo-Fenton slows down a lot.

In any case, the composition of WW is very important because the experiments done with IFAS present a behavior something different than the experiments carried out with the other WW as a matrix. In IFAS it is even more pronounced that dark Fenton, at circumneutral pH, has less weight. In such a way that it lowers very little and then flattens out and therefore does not get to cross with the photo-Fenton at normal pH. In fact, in experiments done with another sample of IFAS, similar behavior was observed but the initial drop was a little more pronounced. In that experiment, which lasted up to 180 minutes, the great slowdown after the initial drop was also observed, when there is a chelating agent. In fact, it was observed that between 30 and 180 min, the concentration of PROP was only reduced by 10% (more information can be found in Figure S3 in Supplementary information). The behavior seems geometrically similar to Milli-Q but it is the opposite. In Milli-Q, the curves (Fig. 7) corresponding to conventional photo-Fenton and photo-Fenton at circumneutral pH do not cross each other because in normal photo-Fenton the dark Fenton is very important and the concentration drops a lot. In fact,

for conventional photo-Fenton, the value of  $k_1$  with Milli-Q was  $1.35 \text{ min}^{-1}$ , this is the highest value for different matrices and approximately 10 times higher than the value for circumneutral pH. The value of  $k_2$  was also the highest. Thus, the reaction rate was very high and the possibility of circumneutral photo-Fenton process to achieve better kinetics was low.

Concerning to the kinetic constants presented in Table 2, another observation can be made.  $k_2$  obtained at circumneutral pH is higher than this one at conventional photo-Fenton for MBR, CAS-NE and CAS, but the contrary occurs with IFAS. Probably, this fact was due to the presence of different organic matter constituents which were not present in MBR sample, even though both came from the same WWTP. Table 3 presents the EfOM composition corresponding to MBR and IFAS samples, analysed by SEC-OCD methodology. In Table 3, it can also be observed EfOM composition corresponding to CAS, which present high organic content (like IFAS) but gives better performance in both photo-Fenton at neutral pH and conventional photo-Fenton. As it can be observed, in all compounds, IFAS presents higher concentrations than MBR and CAS.

**Table 3.** EfOM compositions for MBR and IFAS wastewater samples.

<b>Compounds</b> <b>[<math>\mu\text{gC} \cdot \text{L}^{-1}</math>]</b>	<b>MBR</b>	<b>IFAS</b>	<b>CAS</b>
Biopolymers	51	3392	1611
Humic substances	3319	5217	3916
Building Blocks	1139	1622	1701
Neutrals	1667	3205	3318
Acids	350	789	1140

IFAS has an approximately 70 times higher concentration of biopolymers than MBR, and almost 2 times more of humic substances. Biopolymers and humic substances can chelate the iron present in solution. Thus, probably the explanation of the different trend in IFAS than other WW in circumneutral photo-Fenton could be that iron in solution was also chelated by biopolymers or humic substances. This fact could make the efficiency of the process decrease. In addition, IFAS has an approximately 2 times higher concentration of biopolymers than CAS, and 1.3 times more of humic substances. Compared to MBR, the highest difference is in biopolymers since the concentration of humic substances are similar. MBR and CAS showed better results for PROP removal in photo-Fenton catalyzed by EDDS-Fe(II). However, IFAS achieved better PROP degradation in conventional photo-Fenton. Thus, it could be deduced that probably the highest influence on iron chelates is due to humic substances and in a lesser extent to biopolymers.

Coming back again to the different kinetic constants used, it can be seen that, when the matrix is WW and for a given matrix, the values of  $k_2$ ,  $k_3$  and  $k_4$  are not very different from each other. However,  $k_3$  and  $k_4$  show a much worse interpretation of what happens since they do not distinguish the fast initial decrease in PROP concentration due to dark Fenton. On the other hand,  $k_3$  and  $k_4$  allow an easy global approximation to determine the process that allows the highest rate in the global reduction of the PROP concentration.

To conclude this section the results of biodegradability for photo-Fenton catalyzed by EDDS-Fe(II) are shown in Figure 8. These results are presented as a percentage of BOD increase after the photo-Fenton treatment.

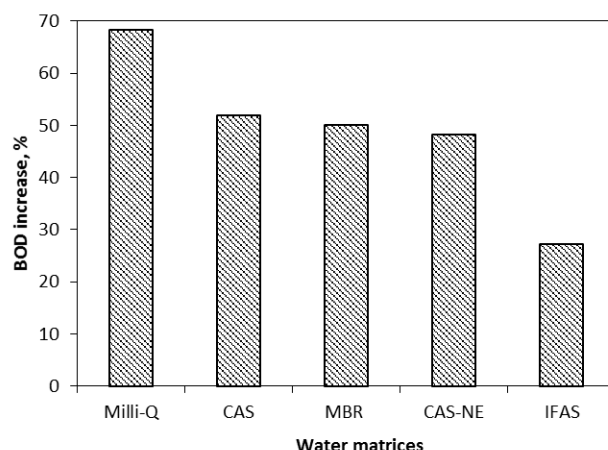


**Figure 8.** Percentage of BOD increase after treatment of different matrices with a ratio of 1:1 L-Fe(II).  $[\text{PROP}]_0 = 0.19 \text{ mM}$ ;  $[\text{Fe(II)}]_0 = 0.18 \text{ mM}$ ;  $[\text{H}_2\text{O}_2]_0 = 4.41 \text{ mM}$ .

As it can be observed in Fig.8, all matrices demonstrated an increase of BOD after the treatment. Moreover, in supplementary material (Table S2) it can be found the initial values of BOD, COD and biodegradability. Milli-Q water shows the best results (near 70%) and IFAS the worst ones (approximately 30%). CAS, MBR and CAS-NE gave close results (approximately 50%).

In Milli-Q water the solution is the most biodegradable due to almost all the PROP was removed (99.6%). Thus, the intermediates formed could be oxidized during the photo-Fenton treatment. Therefore, the structures of remaining intermediates at 60 minutes probably were more simple than in the other matrices increasing the BOD. In addition, as it can be seen in figure 6, the iron remaining in solution is higher in Milli-Q than other matrices. Thus, there is more chelating agent (EDDS) in solution and, as EDDS is considered biodegradable, this could also increase the biodegradability. Regarding CAS and CAS-NE the results were very close. On the other hand, MBR showed similar results

than CAS-NE because both present a similar PROP degradation (62.7% for MBR and 61.0% for CAS-NE). The two wastewaters present values of TOC very close too. So that, the organic matter to oxidize in the BOD analysis is probably the same in the two WW. Finally, IFAS presented a lower percentage of increase of biodegradability, because only a 14.3% of PROP removal was achieved. In addition, IFAS is an effluent of secondary treatment and its content on biodegradable organic matter is lower.

The increase in biodegradability suggests that the oxidation intermediates are becoming simpler structures. In this work the main oxidation intermediates of propranolol were not analyzed. However, some articles in the literature and previous works in our laboratory detected the main intermediates of propranolol and its pathways [11, 58-62]. Moreover, in table S3 in supplementary material the structures of main oxidation intermediates of propranolol detected in our previous works can be found [61, 62].

#### **4. Conclusions**

In this study, the degradation of PROP by conventional photo-Fenton with BLB and UV-A LED radiation was compared. The results indicated that, using ultrapure water, the differences were not significant. However, with WW matrices the differences increase mainly due to the presence of different organic matter which absorbs part of radiation and also compete with PROP for hydroxyl radicals. Turbidity also influences on the radiation transfer through the photoreactor. In addition, PROP removal decreases when TOC of WW increases. Thus, ultrapure water achieved the best PROP degradation while IFAS presented the worst PROP removal.

Two molar ratios L-Fe (1:1 and 1.5:1) and two chelating agents (EDDS and EDTA) were tested. EDDS as a chelating agent with 1:1 L-Fe molar ratio gave the best results in PROP degradation, biodegradability and toxicity.



Concerning the efficiency in PROP degradation, experiments of photo-Fenton at circumneutral pH showed the same trend than experiments of conventional photo-Fenton for the different matrices. Comparing photo-Fenton at acid PH and circumneutral pH, IFAS and ultrapure water achieved higher PROP removals with conventional photo-Fenton but MBR, CAS and CAS-NE showed the highest PROP degradations for photo-Fenton catalyzed by EDDS-Fe(II). In the case of IFAS the presence of biopolymers and more humic substances, which can chelate with iron, probably affected the PROP degradation and changing the trend of degradation than other WWs.

Dark Fenton is very important during the initial time (30 s) of the experiments. For instance, with Milli-Q water, 50% of PROP is degraded in 30 s. for the other WW matrices, the trend is similar. After the initial 30 s, photo-Fenton controls the process and reaction rate slows down. In the case of photo-Fenton at circumneutral pH, the effect of dark Fenton during the initial 30 s is not so important due to the chelation of  $\text{Fe}^{2+}$ .

### **Acknowledgments**

The authors are appreciative with the Ministry of Science and Innovation of Spain (projects CTQ2014-52607-R and CTQ2017-86466-R), Ministry of Education, Culture and Sports (FPU research fellowship FPU-16/02101), Institute for Water Research (IdRA) of Universitat de Barcelona and AGAUR-Generalitat de Catalunya (project 2014SGR245 and 2017SGR-131) for providing funds for this study.

### **References**

- [1] T.A. Ternes, A. Joss, Human Pharmaceuticals, Hormones and Fragrances. The Challenge of Micropollutants in Urban Water Management, IWA Publishing, London, New York, 2006.

- [2] Y. Lee, U. von Gunten, Oxidative transformation of micropollutants during municipal wastewater treatment: Comparison of kinetic aspects of selective (chlorine, chlorine dioxide, ferrate <sup>VI</sup>, and ozone) and non-selective oxidants (hydroxyl radical), *Water Research* 44 (2010) 555-566.
- [3] M. Ibáñez, V. Borova, C. Boix, R. Aalizadeh, R. Bade, N.S. Thomaidis, F. Hernández, UHPLC-QTOF MS screening of pharmaceuticals and their metabolites in treated wastewater samples from Athens, *Journal of Hazardous Materials* 323 (Part A) (2017) 26–35.
- [4] M. Gros, K.M. Blum, H. Jernstedt, G. Renman, S. Rodríguez-Mozaz, P. Haglund, P.L. Andersson, K. Wiberg, L. Ahrens, Screening and prioritization of micropollutants in wastewaters from on-site sewage treatment facilities, *Journal of Hazardous Materials* 328 (2017) 37–45.
- [5] R. P. Deo, Pharmaceuticals in the surface water of the USA: A review, *Current Environmental Health Reports* 1 (2014) 113-122.
- [6] N. De la Cruz, J. Giménez, S. Esplugas, D. Grandjean, L.F. de Alencastro, C. Pulgarin, Degradation of 32 emergent contaminants by UV and neutral photo-Fenton in domestic wastewater effluent previously treated by activated sludge, *Water Research* 46 (2012) 1947-1957.
- [7] A. Pal, K.Y.H. Gin, A.Y.C. Lin, M. Reinhard, Impacts of emerging organic contaminants on freshwater resources: review of recent occurrences, sources, fate and effects, *Science of the Total Environment* 408 (2010) 6062-6069.
- [8] L.H.M.L.M. Santos, A.N. Araujo, A. Fachini, A. Pena, C. Delerue- Matos, M.C.B.S.M. Montenegro, Ecotoxicological aspects related to the presence of

pharmaceuticals in the aquatic environment, *Journal of Hazardous Materials* 175 (2010) 45-95.

[9] N. De la Cruz, L. Esquiús, D. Grandjean, A. Magnet, A. Tungler, L.F. de Alencastro, C. Pulgarin, Degradation of emergent contaminants by UV, UV/H<sub>2</sub>O<sub>2</sub> and neutral photo-Fenton at pilot scale in a domestic wastewater treatment plant, *Water Research* 47 (2013) 5836-5845.

[10] J. Maszkowska, S. Stolte, J. Kumirska, P. Łukaszewicz, K. Mioduszevska, A. Puckowski, M. Caban, M. Wagil, P. Stepnowski, A. Białk-Bielinska, Beta-blockers in the environment: Part I. Mobility and hydrolysis study, *The Science of the Total Environment* 493 (2014) 1112–1121.

[11] S.O. Ganiyu, N. Oturan, S. Raffy, G. Esposito, E. D. van Hullesbusch, M. Cretin, M.A. Oturan, Use of Sub-stoichiometric Titanium Oxide as a Ceramic Electrode in Anodic Oxidation and Electro-Fenton Degradation of the Beta-blocker Propranolol: Degradation Kinetics and Mineralization Pathway, *Electrochimica Acta* 242 (2017) 344-354.

[12] C. Fernández, M. González-Doncel, J. Pro, G. Carbonell, J.V. Tarazona, Occurrence of pharmaceutically active compounds in surface waters of the henares-jarama-tajo river system (madrid, spain) and a potential risk and characterization, *The Science of the Total Environment* 408 (2010) 543-551.

[13] K. Kümmerer, Drugs in the environment: emission of drugs, diagnostic aids and disinfectants into wastewater by hospitals in relation to other sources: a review, *Chemosphere* 45 (2001) 957–969.

- [14] M. Gros, M. Petrovic, D. Barceló, Development of a multi-residue analytical methodology based on liquid chromatography-tandem mass spectrometry (LC-MS/MS) for screening and trace level determination of pharmaceuticals in surface and wastewaters, *Talanta* 70 (2006) 678-690.
- [15] V. Gabet-Giraud, C. Miège, J.M. Choubert, S.M. Ruel, M. Coquery, Occurrence and removal of estrogens and beta blockers by various processes in wastewater treatment plants, *The Science of the Total Environment* 408 (2010) 4257-4269.
- [16] S. Terzic, I. Senta, M. Ahel, M. Gros, M. Petrovic, D. Barceló, J. Müller, T. Knepper, I. Martí, F. Ventura, P. Jovancic, D. Jabucar, Occurrence and fate of emerging wastewater contaminants in Western Balkan Region, *The Science of the Total Environment* 399 (2009) 66-77.
- [17] Y. Yang, J. Fu, H. Peng, L. Hou, M. Liu, J.L. Zhou, Occurrence and phase distribution of selected pharmaceuticals in Yangtze Estuary and its costal zone, *Journal of Hazardous Materials* 190 (2011) 588-596.
- [18] D.B. Huggett, B.W. Brooks, B. Peterson, C.M. Foran, D. Schlenk, Toxicity of select beta adrenergic receptor-blocking pharmaceuticals (b-blockers) on aquatic organisms, *Arch. Environ. Contam. Toxicol.* 43 (2002) 229–235
- [19] J.J. Pignatello, Y. Sun, Complete oxidation of metolachlor and methyl parathion in water by the photoassisted Fenton reaction, *Water Research* 29 (1995) 1837–1844.
- [20] J.M. Monteagudo, A. Duran, C. Lopez-Almodovar, Homogeneous ferrioxalate assisted solar photo-Fenton degradation of Orange II aqueous solutions, *Applied Catalysis B* 83 (2008) 46–55.

- [21] E. Evgenidou, I. Konstantinou, K. Fytianos, I. Poullos, Oxidation of two organophosphorus insecticides by the photo-assisted Fenton reaction, *Water Research* 41 (2007) 2015–2027.
- [22] F. Méndez-Arriaga, S. Esplugas, J. Giménez, Degradation of the emerging contaminant ibuprofen in water by photo-Fenton, *Water Research* 44 (2010) 589–595.
- [23] R.G. Zepp, B.C. Faust, J. Hoigné, Hydroxyl radical formation in aqueous reactions (pH 3–8) of iron(II) with hydrogen peroxide: the photo-Fenton reaction, *Environmental Science and Technology* 26 (1992) 313–319.
- [24] M. Fukushima, K. Tatsumi, S. Nagao, Degradation characteristics of humic acid during photo-Fenton processes, *Environmental Science and Technology* 35 (2001) 3683–3690.
- [25] J.J. Pignatello, G. Chapa, Degradation of PCBs by ferric ion, hydrogen peroxide and UV light, *Environmental Toxicology and Chemistry* 13 (1994) 423–427.
- [26] S. Miralles-Cuevas, D. Darowna, A. Wanag, S. Mozia, Malato S, I. Oller, Comparison of UV/H<sub>2</sub>O<sub>2</sub>, UV/S<sub>2</sub>O<sub>8</sub><sup>2-</sup>, solar/Fe(II)/H<sub>2</sub>O<sub>2</sub> and solar/Fe(II)/S<sub>2</sub>O<sub>8</sub><sup>2-</sup> at pilot plant scale for the elimination of micro-contaminants in natural water, *Chemical Engineering Journal* 310 (2017) 514–524.
- [27] I. De la Odra, L. Ponce-Robles, S. Miralles-Cuevas, I. Oller, S. Malato, J.A. Sánchez Pérez, Microcontaminant removal in secondary effluents by solar photo-Fenton at circumneutral pH in raceway pond reactors, *Catalysis Today* 287 (2017) 10–14.
- [28] J.J. Pignatello, E. Oliveros, A. McKay, Advanced oxidation processes for organic contaminant destruction based on the Fenton reaction and related chemistry, *Crit. Rev. Environmental Science and Technology* 36 (2006) 1–84.

- [29] S. Miralles-Cuevas, I. Oller, A. Ruiz-Delgado, A. Cabrera-Reina, L. Cornejo-Ponce, S. Malato, EDDS as complexing agent for enhancing solar advanced oxidation processes in natural water: Effect of iron species and different oxidants, *Journal of Hazardous Materials*, <https://doi.org/10.1016/j.jhazmat.2018.03.018>.
- [30] A. De Luca, R. F. Dantas, S. Esplugas, Assessment of iron chelates efficiency for photo-Fenton at neutral pH, *Water Research* 61 (2014) 232-242.
- [31] W. Huang, M. Brigante, F. Wu, K. Hanna, G. Mailhot, Development of a new homogenous photo-Fenton process using Fe(II)-EDDS complexes, *Journal of Photochemistry and Photobiology A: Chemistry* 239 (2012) 17-23.
- [32] I. De la Obra, B. Esteban García, J.L. García Sánchez, J.L. Casas López, J.A. Sánchez Pérez, Low cost UVA-LED as a radiation source for the photo-Fenton process: a new approach for micropollutant removal from urban wastewater, *Photochemical & Photobiological Sciences* 16 (2017) 72-78.
- [33] A.C. Chevremont, A.M. Farnet, M. Sergent, B. Columb, Effect of coupled UV-A and UV-C LEDs on both microbiological and chemical pollution of urban wastewaters, *Science of Total Environment* 426 (2012) 304-310.
- [34] O. Autin, C. Romelot, L. Rust, J. Hart, P. Jarvis, J. MacAdam, S.A. Parsons, B. Jefferson, Evaluation of a UV-light emitting diodes unit for the removal of micropollutants in water for low energy advanced oxidation processes, *Chemosphere* 92 (2013) 745-751.
- [35] P. Xiong, J. Hu, Degradation of acetaminophen by UVA/LED/TiO<sub>2</sub> process, *Separation and Purification Technology* 91 (2012) 89-95.

- [36] S. Verma, M. Sillanpää, Degradation of anatoxin-a by UV-C LED and UV-C LED/H<sub>2</sub>O<sub>2</sub> advanced oxidation processes, *Chemical Engineering Journal* 274 (2015) 274-281.
- [37] R.J. Tayade, T.S. Natarajan, H.C. Bajaj, Photocatalytic degradation of methylene blue dye using ultraviolet light emitting diodes, *Industrial & Engineering Chemistry Research* 48 (2009) 10262-10267.
- [38] M.A. Würtele, T. Kolbe, M. Lipsz, A. Külberg, M. Weyers, M. Kneissl, M. Jekel, Application of GaN-based ultraviolet-C light emitting diodes-UV-LEDs-for water disinfection, *Water Research* 45 (2011) 1481-1489.
- [39] G. Matafonova, V. Batoev, Recent advanced in application of UV light-emitting diodes for degrading organic pollutants in water through advanced oxidation processes: A review, *Water Research* 132 (2018) 177-189.
- [40] N.F.F. Moreira, J.M. Sousa, G. Macebo, A.T. Ribeiro, L. Barrientos, M. Pedrosa, J.L.Faria, F.R.Pereira, S.Castro-Silva, M.A.Segundo, C.M.Manaia, O.C. Nunes, A.M.T.Silva, Photocatalytic ozonation of urban wastewater and surface water using immobilized TiO<sub>2</sub> with LEDs: Micropollutants, antibiotic resistance genes and estrogenic activity, *Water Research* 94 (2016) 10-22.
- [41] M.H. Rasoulifard, M. Fazli, M.R. Eskandarian, Performance of the light-emitting diodes in a continuous photoreactor for degradation of Direct Red using UV-LED/S<sub>2</sub>O<sub>8</sub><sup>2-</sup> process, *Journal of Industrial & Engineering Chemistry* 24 (2015) 121-126.
- [42] R.F. Pupo Nogueira, M.C. Oliveira, W.C. Paterlini, Simple and fast spectrophotometric determination of H<sub>2</sub>O<sub>2</sub> in photo-Fenton reactions using metavanadate, *Talanta* 66 (2005) 86-89.

- [43] A.D. Eaton, L.S. Clesceri, A.E. Greenberg, M.A.H. Franson, Standard Methodes for the Examination of Water and Wastewater, twenty-first ed. (2005) APA-AWWA-WEE.
- [44] S.A. Huber, A. Balz, M. Abert, W. Pronk, Characterization of aquatic humic and non-humic matter with size-exclusion chromatography-organic carbon detection-organic nitrogen detection (LC-OCD-OND), *Water Research* 45 (2011) 879-885.
- [45] S. Giannakis, F. A. Gamarra Vives, D. Grandjean, A. Magnet, L. F. De Alencastro, C. Pulgarin, Effect of advanced oxidation processes on the micropollutants and the effluent organic matter contained in municipal wastewater previously treated by three different secondary methods, *Water Research* 84 (2015) 295-306.
- [46] D. Schowanek, T.C.J. Feijtel, C.M. Perkins, F.A. Hartman, T.W. Federle, R.J. Larson, Biodegradation of [S,S], [R,R] and mixed stereoisomers of ethylene diamine disuccinic acid (EDDS), a transition metal chelator, *Chemosphere* 34 (11) (1997) 2375–2391.
- [47] J.D. Englehardt, D.E. Meeroff, L. Echevoyen, Y. Deng, F.M. Raymo, T. Shibata, Oxidation of aqueous EDTA and associated organics and coprecipitation of inorganics by ambient iron-mediated aeration, *Environmental Science and Technology* 41 (2006) 270–276.
- [48] S. Metsarinne, T. Tuhkanen, R. Aksela, Photodegradation of ethylenediaminetetraacetic acid (EDTA) and ethylenediamine disuccinic acid (EDDS) within natural UV radiation range, *Chemosphere* 45 (2001) 949–955.
- [49] J. Li, 17 $\beta$ -Estradiol Degradation Photoinduced by Iron Complex, Clay and Iron Oxide Minerals: Effect of the Iron Complexing Agent Ethylenediamine-



Ethylenediamine-N, N- Disuccinic Acid, University Blaise Pascal, Aubière, 2010, PhD Thesis.

[50] W. Huang, M. Brigante, F. Wu, C. Mousty, K. Hanna, G. Mailhot, Assesment of the Fe(III)-EDDS complex in Fenton-Like process: from the radical formation to the degradation of bisphenol A, *Environmental Science & Technology* 47 (2013) 1952-1959.

[51] B.H.J. Bielski, D.E. Cabelli, R.L. Arudi, A.B. Ross, Reactivity of  $\text{HO}_2/\text{O}_2^-$  radicals in aqueous solution, *Journal of Physical and Chemical Reference Data* 14 (1985) 1041–1100.

[52] G. V. Buxton, C. L. Greenstock, W. P. Helman, A. B. Ross, Critical review of rate constants for reactions of hydrated electrons, hydrogen atoms and hydroxyl radicals ( $\cdot\text{OH}/\cdot\text{O}$ ) in aqueous solution, *Journal of Physical and Chemical Reference Data* 17 (2) (1988) 513-883.

[53] J. Benner, E. Salhi, T. Ternes, U. von Gunten, ozonation of reverse osmosis concentrate: kinetics and efficiency of beta blocker oxidation, *Water Research* 42 (2008) 3003-3012.

[54] D. Vione, M. Minella, V. Maurino, C. Minero, Indirect photochemistry in sunlit surface waters: photoinduced production of reactive transient species, *Chemistry: A European Journal* 20 (2014) 10590-10606.

[55] J. Mack, J. R. Bolton, Photochemistry of nitrite and nitrate in aqueous solution: a review. *Journal of Photochemistry and Photobiology A: Chemistry* 128 (1-3) (1999) 1-13.

- [56] S. Goldstein, J. Rabani, Polychromatic UV photon irradiance measurements using chemical actinometers based on  $\text{NO}_3^-$  and  $\text{H}_2\text{O}_2$  excitation: Applications for industrial photoreactors, *Environmental Science and Technology* 42 (9) (2008) 3248-3253.
- [57] Y. F. Ji, C. Zeng, C. Ferronato, J. M. Chovelon, X. Yang, Nitrate-induced photodegradation of atenolol in aqueous solution: kinetics, toxicity and degradation pathways, *Chemosphere* 88 (2012) 644-649.
- [58] T. Chen, J. Ma, Q. Zhang, Z. Xie, Y. Zeng, R. Li, H. Liu, Y. Liu, W. Lv, G. Liu, Degradation of propranolol by UV-activated persulfate oxidation: Reaction kinetics, mechanisms, reactive sites, transformation pathways and Gaussian calculation, *Science of the Total Environment* 690 (2019) 878-890.
- [59] E. Marco-Urrea, J. Radjenovic, G. Caminal, M. Petrovic, T. Vicent, D. Barceló, Oxidation of atenolol, propranolol, carbamazepine, and clofibric acid by biological Fenton-like system mediated by the white-rot fungus *Trametes versicolor*, *Water Research* 44 (2010) 521-532.
- [60] E. Cuervo Lumbaque, R.M. Cardoso, A. Dallegrave, L.O. dos Santos, M. Ibáñez, F. Hernández, C. Sirtori, Pharmaceutical removal from different water matrixes by Fenton process at near-neutral pH: Doehlert design and transformation products identification by UHPLC-QTOF MS using a purpose-built database, *Journal of Environmental Chemical Engineering* 6 (2018) 3951-3961.
- [61] N. De la Cruz, Estudio de la eliminación de contaminantes emergentes en aguas mediante procesos de oxidación avanzados, *Doctoral Thesis*, University of Barcelona, 2013 ([http://diposit.ub.edu/dspace/bitstream/2445/66864/1/NDLCG\\_TESIS.pdf](http://diposit.ub.edu/dspace/bitstream/2445/66864/1/NDLCG_TESIS.pdf) and <http://hdl.handle.net/2445/66864>).

[62] V. Romero, N. De la Cruz, R.F. Dantas, P. Marco, J. Giménez y S. Esplugas, Photocatalytic Treatment of Metoprolol and Propranolol, *Catalysis Today* 161 (2011) 115-120.

## Supplementary Information for

### Micropollutants removal in real WW by photo-Fenton (circumneutral and acid pH) with BLB and LED lamps

N. López-Vinent, A. Cruz-Alcalde, C. Gutiérrez, P. Marco, J. Giménez\*, S. Esplugas

Department of Chemical Engineering and Analytical Chemistry, Faculty of Chemistry, Universitat de Barcelona, C/Martí i Franqués 1, 08028 Barcelona, Spain.

\*Corresponding author:

Jaime Giménez Farreras, phone: +34 934021293 e-mail: j.gimenez.fa@ub.edu

### Table of Contents

Biochemical Oxygen Demand: Brief explanation of the process.....	p.2
<b>Figure S1.</b> Reactor illumination with two radiation sources.....	p.2
<b>Figure S2.</b> Hydrogen peroxide monitoring for different WW in conventional photo-Fenton and photo-Fenton catalyzed by EDDS-Fe(II) using LEDs.....	p.3
<b>Figure S3.</b> Degradation of PROP by conventional photo-Fenton (CPF) and photo-Fenton catalyzed with EDDS with another sample of IFAS.....	p.3
<b>Table S1.</b> Characteristics of dissolved effluent organic matter (EfOM) fractions.....	p.4
<b>Table S2.</b> Initial values of BOD, COD and biodegradability for different wastewaters and Milli-Q.....	p.4
<b>Table S3.</b> Main oxidation intermediates of propranolol identified by N. de la Cruz [61].....	p.5

**Biochemical Oxygen Demand: Brief explanation of the process.**

The Biochemical Oxygen Demand was evaluated according to the 5210-standard method. This method consists on filling with seeded and nourished sample an airtight bottle of specified size (500 mL, appropriated for OxyTop), which is incubated at the specified temperature (20 °C) for 5 days.

The measurement was done by OxyTop whose mechanism is based on the pressure variation in a closed system. The present microorganisms in the sample consume oxygen and generate CO<sub>2</sub> because of their metabolic activity. This CO<sub>2</sub> is absorbed with NaOH and then a pressure drop is produced, which is related to oxygen concentration and BOD. The biodegradability was calculated according to equation S1, at the beginning and at the end of the experiment. The increase in the biodegradability is estimated by eq. S2, where “*f*” is at the end of the experiment and “*i*” is the biodegradability at initial time.

$$\text{Biodegradability} = \frac{DBO}{COD} \quad (\text{S1})$$

$$\% \text{ increase biodegradability} = \left( \frac{\text{Biodegradability}_f - \text{Biodegradability}_i}{\text{Biodegradability}_f} \right) \times 100 \quad (\text{S2})$$

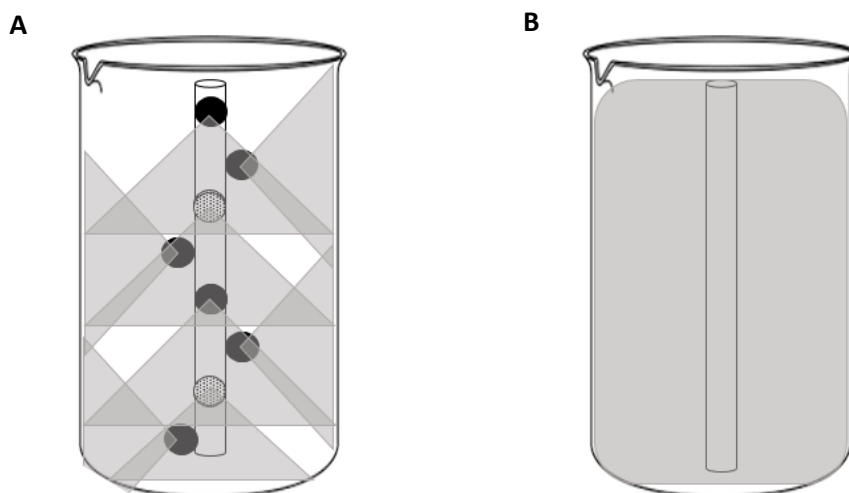


**Figure S1.** Reactor illumination with two radiation sources. A) UV-A LED 8W; B) BLB 8W.

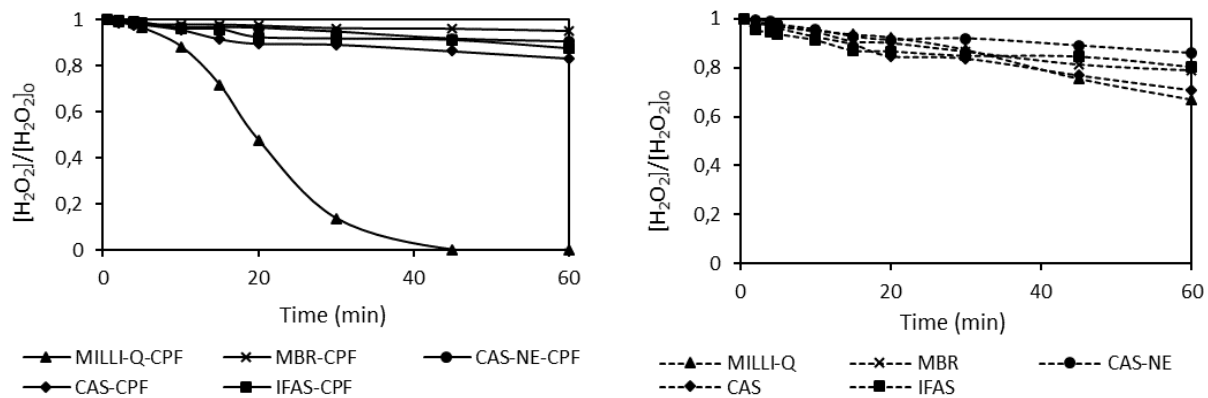


**Figure S2.** Hydrogen peroxide monitoring for different WW in conventional photo-Fenton (CPF) and photo-Fenton catalyzed by EDDS-Fe(II) using LEDs.

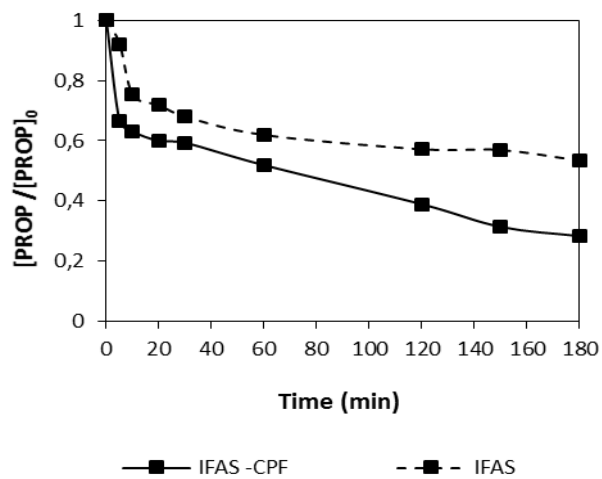


**Figure S3.** Degradation of PROP by conventional photo-Fenton (CPF) and photo-Fenton catalyzed with EDDS with another sample of IFAS

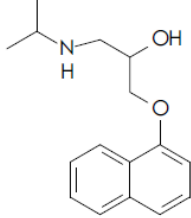
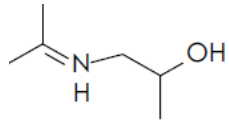
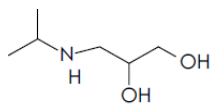
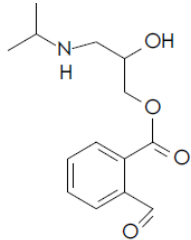
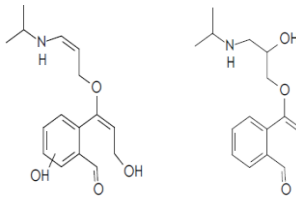
**Table S1.** Characteristics of dissolved effluent organic matter (EfOM) fractions

<b>EfOM fractions</b>	<b>Description</b>
Biopolymers	Amino acids and proteins
Humic substances	Humic/fluvic acids and hydrophobic humics
Building Blocks	Intermediates of humic substances
Low molecular weight neutrals	Non-acidic intermediates (alcohols, ketones..)
Low molecular weight acids	Intermediates of organics

**Table S2.** Initial values of BOD, COD and biodegradability for different wastewaters and Milli-Q.

	<b>BOD</b> <b>(mg O<sub>2</sub> ·L<sup>-1</sup>)</b>	<b>COD</b> <b>(mg O<sub>2</sub> ·L<sup>-1</sup>)</b>	<b>Biodegradability</b>
Milli-Q	6.4	105.0	0.061
MBR	10.6	100.2	0.106
CAS-NE	16.5	100.0	0.165
CAS	16.0	125.3	0.128
IFAS	13.6	127	0.107

**Table S3.** Main oxidation intermediates of propranolol identified by N. de la Cruz [61].

Compound	m/z (+)	Molecular formula	Structure
Propranolol	260	C <sub>16</sub> H <sub>21</sub> NO <sub>2</sub>	
PROP <sub>I</sub>	116	C <sub>6</sub> H <sub>13</sub> NO	
PROP <sub>II</sub>	134	C <sub>6</sub> H <sub>15</sub> NO <sub>2</sub>	
PROP <sub>III</sub>	266	C <sub>14</sub> H <sub>19</sub> NO <sub>4</sub>	
PROP <sub>IV</sub>	292	C <sub>16</sub> H <sub>21</sub> NO <sub>4</sub>	
PROP <sub>V</sub>	308	C <sub>16</sub> H <sub>21</sub> NO <sub>5</sub>	